Peripheral T-cell lymphoma cell line T8ML-1 highlights conspicuous targeting of PVRL2 by t(14;19)(q11.2;q13.3)

Focal amplifications and chromosome translocations involving the long arm of chromosome 19 (19q13.3) are recurrent in T-cell lymphoma, where neighboring *BCL3* and *PVRL2* are competing target genes. Here we present the oncogenomic characterization of a peripheral T-cell lymphoma (PTCL) cell line T8ML-1 to reveal t(14;19)(q11.2;q13.3) juxtaposing *TRA@* and *PVRL2*. Parallel mRNA and protein expression data for the 19q13.3 region of interest pinpointed *PVRL2* as the sole conspicuous target therein. Collectively, our findings endorse T8ML-1 as the first proven cell line model for t(14;19)/ PTCL.

PTCL form a varied group of poor prognosis diseases

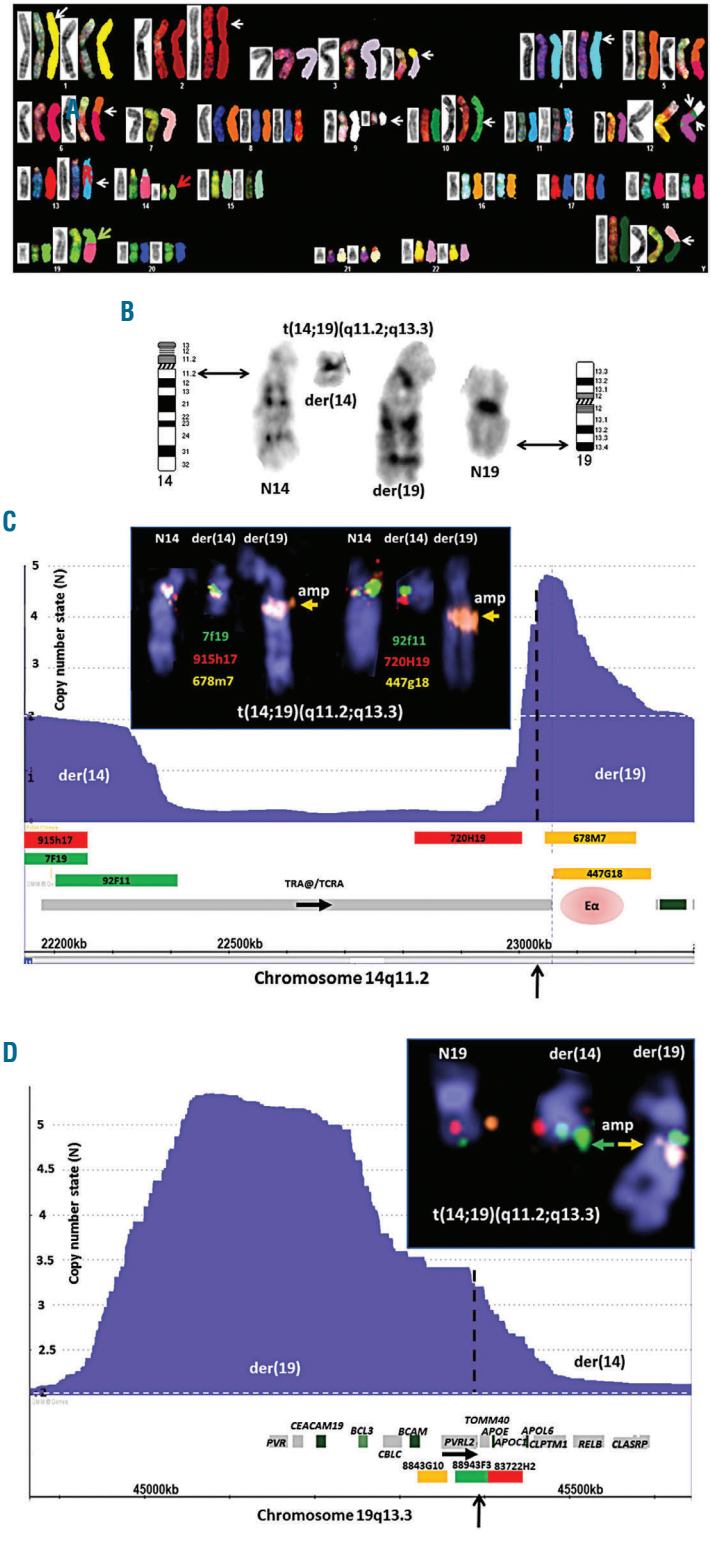

Figure 1. Genomic characteristics of t(14;19)(q11.2;q13.3) in T8ML-1. (A) Spectral karyotyping (SKY) depicts (left-to-right) G-banded, unprocessed and pseudocolored chromosome images from the T8ML-1 karyotype showing multiple alterations. Red and green arrows indicate, respectively, der(14) and der(19) translocation partners; white arrows show non-participant breakpoints. SKY revealed a heterogeneous but stable clonal substructure consistent with persistent patient-derived subclones *in vitro*. (B) G-banding shows breakpoints of t(14;19) at 14q11.2 and 19q13.3. (C/D) Cytoscan plots for 14q11.2 (C) and 19q13.3 (D) show genomic copy number plots. Figure insets show fluorescence *in situ* hybridization (FISH) using tilepath clones together with mapping data for BAC (C) and fosmid (D) clones. Note breakpoint assignments based on FISH images depicting 14q11.2 and 19q13.3 breakpoints lying at/near *TRA@* downstream enhancer and downstream short-form *PVRL2*, respectively. Discrepant signal strengths correspond to focal amplification as shown by copy number plots for both loci. FISH and genomic arrays were performed as described previously. Cytogenetic images were captured using a HiSKY system (Applied Spectral Imaging, Edingen, Germany) configured to an Axioimager D1 microscope (Zeiss, Jena, Germany). Clones were kindly donated by the Siebert Lab as described in ref. 10, or purchased from BACPAC Resources, Children's Hospital, Oakland, CA, USA, and labeled by nick translation with dUTP fluors Dy495 (green), Dy590 (red) and Dy547 (yellow) purchased from Dyomics, Jena, Germany. Genomic array data were provided by Cytoscan High Density genomic arrays (Affymetrix, Thermo Fischer, Darmstadt, Germany).

comprising 10-15% of non-Hodgkin lymphomas. PTCL have proven difficult to classify, due partly to the dearth of biomarkers.[1] PTCL not otherwise specified (NOS) forms the major subgroup, comprising approximately 30% of patients. Responses to current treatment protocols have proven neither particularly effective nor durable with progression-free survival rates of 40-50%. Hence, novel therapies, such as those targeting histone deacetylases, the folate inhibitor pralatrexate, and monoclonal antibodies targeting CCR4, CD4, CD52 plus immunomodulatory drugs and proteasome inhibitors are undergoing evaluation.[2] The search for therapeutic targets is hindered not least by the absence of proven PTCL-NOS cell line models.

Few recurrent oncogenomic alterations have been identified in PTCL. As well as mutations activating the

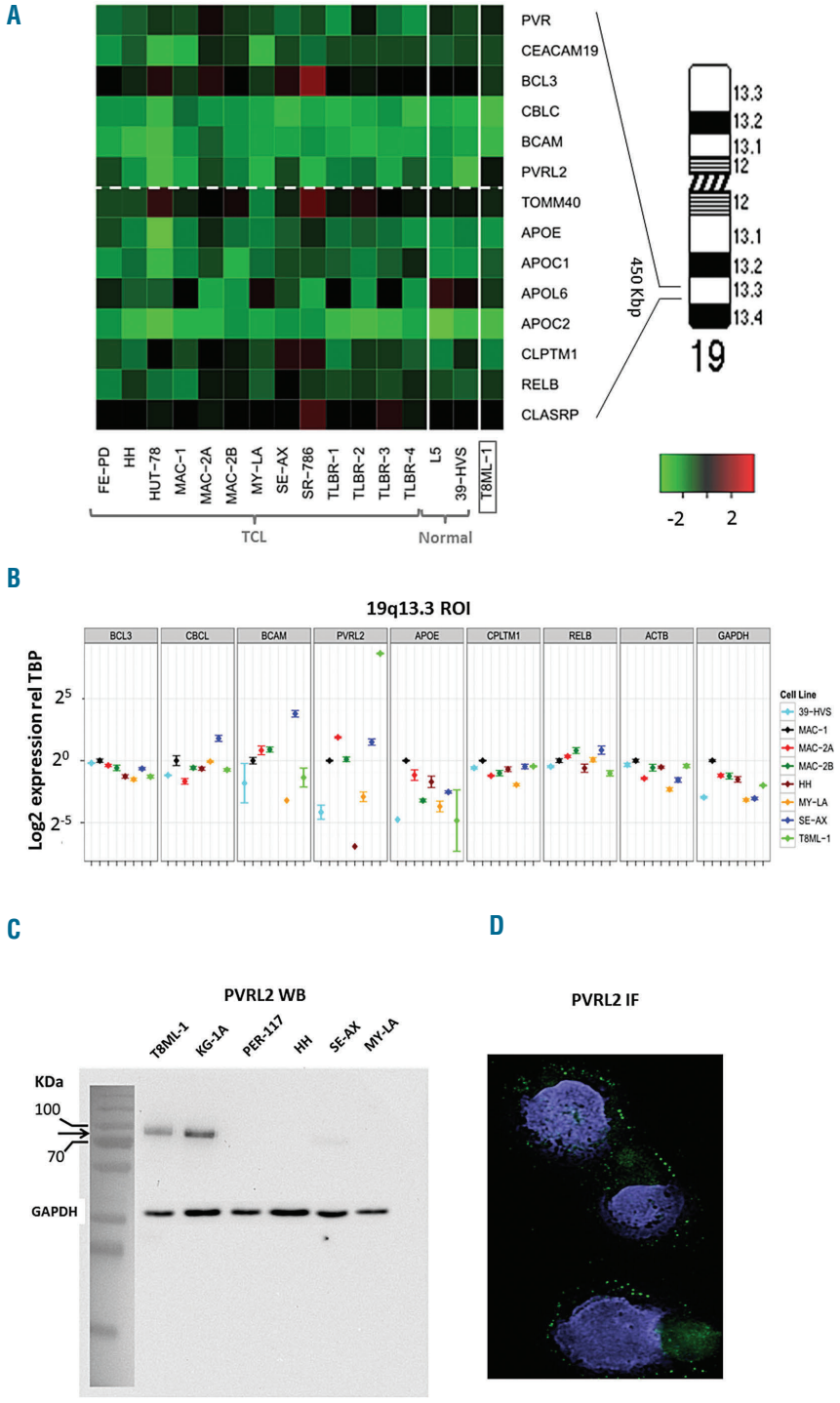

Figure 2. Comparative gene expression at chromosome 19q13.3 in T8ML-1. (A) Heatmap depicts comparative microarray gene expression data for the approximately 450 kbp 19q13.3 region of interest (ROI) in 13 T-cell lymphoma and two normal control cell lines. The breakpoint region is shown by the broken horizontal lines. Note conspicuous, if moderate, expression in T8ML-1 restricted to *PVRL2*, while rival *BCL3* expression remains inconspicuous therein. (B) Shows corresponding quantitative reverse transcripts polymerase chain reaction RqPCR measurement of gene expression at 19q13.3 ROI. Again, only *PVRL2* (short form) evidenced conspicuous and markedly elevated expression in T8ML-1, while *BCL3* remained inconspicuously expressed. Thus, both array and RqPCR data highlight *PVRL2* as the t(14;19) target. Comparison T-cell cell lines were as follows: ALCL: MAC-2A/2B, SR-786; breast implant T-cell lymphoma: TLBR-1/2/3/4; CTCL: FE-PD, HH, HUT-78, MAC-1, MY-LA, SE-AX; normal T cells immortalized spontaneously, L5; or virally, 39-HVS. Additional cell lines were KG-1A (acute myeloid leukemia) and PER-117 (T-cell acute lymphoblastic leukemia). For cell culture details see the DSMZ website (*www.dsmz.de*). Gene expression microarray profiling data were generated using the HG U133 Plus 2.0 gene chip (Affymetrix) or kindly supplied by Prof. Dr. Andreas Rosenwald. For creation of heat maps we used the software CLUSTER version 2.11 and TREEVIEW version 1.60 (http://rana.lbl.gov/EisenSoftware.htm). For RqPCR total RNA was extracted from cell line samples using TRIzol reagent (Invitrogen, Darmstadt, Germany). cDNA was synthesized from 5 μg RNA by random priming using Superscript II (Invitrogen). RqPCR analysis was performed with the 7500 Real-time System, using commercial buffer and primer sets (Applied Biosystems/Life Technologies, Darmstadt, Germany). Quantitative analyses were performed at least twice in triplicate as described previously.[11,12] (C) Western blotting of cell line lysates shows expression of PVRL2 limited to T8ML-1 and the commercial standard cell line KG-1A. GAPDH served as the loading control. Western blotting and immunofluorescence were performed using anti-Nectin 2 antibody EPR6717 (ab125246) purchased from Abcam, Cambridge, UK as described previously.[12] Western blots were generated by the semi-dry method. Protein lysates from cell lines were prepared using SIGMAFast protease inhibitor cocktail (Sigma). Proteins were transferred onto nitrocellulose membranes (Bio-Rad, Munich, Germany) and blocked with 5% dry milk powder dissolved in phosphate-buffered-saline buffer (PBS). (D) Immunofluorescence shows cell surface expression of PVRL2 in T8ML-1 cells.

JAK-STAT pathway, these include the *ALK/NPM1* fusion in anaplastic large cell lymphoma and *ITK/SYK* fusion in follicular PTCL,[3] plus t(14;19)(q11.2;q13) investigated here.[4-7] In the absence of corresponding expression data, the proximity of *BCL3* and *PVRL2* (located ~86 kbp apart) has obscured which (if either) is the true target.

Here, we detail the characterization of a PTCL-derived cell line T8ML-1 with t(14;19) established from a 64-year old female patient diagnosed with fatal PTCL-NOS[8] at both genomic and gene expression levels. T8ML-1 cells were grown in RPMI-1640 medium with 20% fetal bovine serum containing 10 ng/mL interleukin-2 (Sigma-Aldrich, Darmstadt, Germany). DNA profiling of T8ML-1 confirmed authenticity with the following alleles: D5S8-13/13; vWA-16/17; D13S317-8/11; THO1-6/7; TPOX-8/11; D7S820-12/12; D16S539-10/11; CSF1-12/12. Principal component analysis of microarray expression data placed T8ML-1 closest to, but outside cutaneous T-cell lymphoma and Hodgkin lymphoma clusters, i.e. consistent with its singular status (PTCL-NOS) among cell lines (*Online Supplementary Figure S1A*). Hierarchical clustering of T8ML-1 together with public gene expression profiling data[9] showed that T8ML-1 consorts with PTCL patients (*Online Supplementary Figure S1B*) attesting its fitness to model this entity.

Conventional and spectral karyotyping revealed a highly rearranged karyotype bearing t(14;19)(q11.2;q13.3) (Figure 1A,B). Array comparative genomic hybridization revealed multiple gains and losses together with losses of heterozygosity (*Online Supplementary Figure S2A-D*). Coordinates of copy number alterations are given in *Online Supplementary Table S1*, and included biallelic losses at 9p21 (*CDKN2A/B*) and 16q23 (WWOX). Larger copy number alterations were also detected, their breakpoints coinciding with chromosome rearrangements confirming their cytogenetic genesis (Figure 1A).

Fluorescence *in situ* hybridization using end-mapped clones[9] placed respective breakpoints within the *TRA@* locus near the 3´-Eα enhancer at 14q11.2 (Figure 1C), and at 19q3.3 centrally within fosmid clone 8894F3 which straddles the region between 3´-*PVRL2* and *TOMM40* (Figure 1D). Consistent fluorescence *in situ* hybridization signal strength discrepancies revealed co-amplification of the juxtaposed *TRA@* and *BCL3/PVRL2* loci (Figure 1C,D). Array comparative genomic hybridization data confirmed focal amplification at both loci, the 19q13.3 amplicon covering *PVRL2* and the immediately centromeric region extending to *PVR*, together with 3´-*TRA@* including the downstream Eα enhancer. Although the *BCL3-PVRL2* region was genomically amplified, the peak lay ~200 kbp centromeric of the cytogenetic breakpoint. Thus T8ML-1 bears t(14;19)(q11.2;q13.3) canonical in PTCL-NOS amplified 3- to 5-fold, raising the possibility that recurrent *BCL3-PVRL2* amplifications in PTCL4 may mask concurrent chromosome rearrangements.

To refine the 19q13.3 region of interest targetome, T8ML-1 gene expression profiling data were compared with those of 15 analogous cell lines, comprising 13 T-cell lymphoma-derived lines and two from normal T cells. In the T8ML-1 region of interest only *PVRL2* expression topped all cell lines, while its breakpoint-neighbor *TOMM40* and rival *BCL3* were, respectively, inconspicuously and weakly expressed (Figure 2A). Comparison with public gene expression profiling data[9] confirmed *PVRL2* activation in two anaplastic large cell lymphomas and in one PTCL patient, while BCL3 expression in PTCL undercut levels in anaplastic large cell lymphoma and primary T cells (*Online Supplementary Figure S3*). Thus even moderate *PVRL2* activation occurs only sporadically in PTCL, while *BCL3* is usually downregulated.

To validate microarray data quantitative reverse-transcriptase polymerase chain reaction analysis was performed. This confirmed conspicuous upregulation of *PVRL2* in T8ML-1, while expression of *BCL3* and other genes in the region of interest remained nondescript,

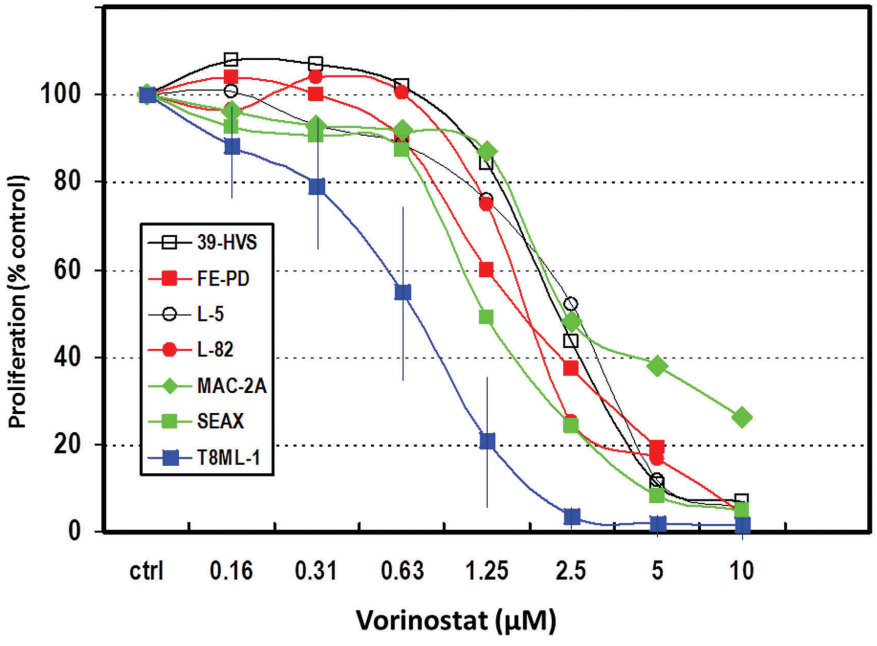

Figure 3. Inhibitory effects of vorinostat. To test the sensitivity of T8ML-1 cells to histone deacetylase inhibition, proliferation responses to vorinostat were compared to those of other T-cell lines by MTT [3-(4,5-dimethylthiazol-2-yl)-2,5-diphenyltetrazolium bromide] assay as described previously.[11] MTT responses show dose-dependent inhibition of T8ML-1 ahead of other T-cell lines, including those established from cutaneous T-cell lymphoma in which vorinostat has been shown to be effective. Assays were performed over 72 h at the doses indicated and repeated at least twice replicated 5-fold. Error bars omitted for clarity. Cell lines were as follows: anaplastic large-cell lymphoma, L-82, MAC-2A; cutaneous T-cell lymphoma, FE-PD, SE-AX; normal T-cell, 39-HVS, L-5.

again spotlighting *PVRL2* (Figure 2B). Protein expression of PVRL2 was investigated by comparative western blotting of T8ML-1 and a positive control (acute myeloid leukemia) cell line, KG-1A, together with four T-cell lymphoma derivates (Figure 2C). This confirmed that neoplastic protein expression of PVRL2 in T-cell entities was restricted toT8ML-1.

PVRL2 (alias *CD112/NECTIN2/PRR2/PVRR2*) encodes a membrane glycoprotein, and immunofluorescence staining confirmed positive membrane expression in T8ML-1 (Figure 2D). This result was supported by flow cytometry data showing cell surface expression comparable to that of positive control KG-1A cells (*Online Supplementary Figure S4*). Thus, the collective genomic and gene expression data pinpoint *PVRL2* as the sole conspicuous target of t(14;19)(q11.2;q13.3) in the PTCL-NOS model T8ML-1, in which it is well expressed as a cell surface membrane component.

Comparative global microarray profiling was also used to mine transcriptional data for clues to pathway activation and potential therapeutic targets. STRING analysis of protein interactions (*http://string-db.org/cgi/network.pl*) of 500 top up/down-regulated genes in T8ML-1 *versus* 13 T-cell lymphoma lines revealed close networking (*Online Supplementary Figure S5*) and significant enrichment for Gene Ontology terms evoking cell membrane themes (*Online Supplementary Table S2A*); while KEGG-pathways included RAR1 signaling and HTLV-1 infection (*Online Supplementary Table S2B*).

Top 100 significant GSEA ontologies (*http://software.broadinstitute.org/gsea/index.jsp*) (*Online Supplementary Table S3A,B*) common to up/down-regulated gene-sets included several connected to T-cell and plasma membrane receptor signaling, together with histone deacetylase targets (P-UP=1.66x10^{-11}; P-DOWN=172x10^{-11}) - the last indicating a therapeutic avenue successfully tried in cutaneous T-cell lymphoma. Accordingly, proliferative responses of T8ML-1 to the clinically approved histone deacetylase inhibitor vorinostat were compared to those of normal and malignant T cells. Growth assay results showed that T8ML-1 tested most sensitive in this panel which included cutaneous T-cell lymphoma models in which the effectiveness of vorinostat has been proven (Figure 3).

Recent evidence from B-cell lymphomas suggests that *PVRL2* is also likely to be the target of the analogous t(14;19)(q32;q13.3).[13] Simultaneous targeting in B/T cells implies that *PVRL2* may support basic proliferation/survival processes rather than T-cell-specific activities. T8ML-1 cells provide a ready model for investigating the neoplastic role of *PVRL2* at the molecular level.

Here we present parallel genomic and gene expression data on t(14;19) cells, with *PVRL2* emerging as the sole visible target at the 19q13.3 region of interest. Although several anaplastic large cell lymphoma and cutaneous T-cell lymphoma cell lines are used widely, T8ML-1 is the first PTCL-NOS candidate encountered by the DSMZ fulfilling basic authentication, mycoplasma testing and viability criteria. Since patient-origin is alone insufficient, the presence of t(14;19)/*TRCA@-PVRL2* hallmarks T8ML-1 as a *bona fide* PTCL-NOS model. Moreover, t(14;19)(q11.2;q13.3) is only the third PTCL translocation modeled in cell lines, alongside t(2;5)/*NPM1-ALK* and t(8;9)/*PCM1-JAK2*.[12] T8ML-1 thus forms a singular preclinical tool for investigating the molecular pathology of this intractable entity for searching actionable targets and testing novel therapies directed against them.

Stefan Ehrentraut,[1] Stefan Nagel,[1] Claudia Pommerenke,[1] Wilhelm G. Dirks,[1] Hilmar Quentmeier,[1] Maren Kaufmann,[1] Corinna Meyer,[1] Margarete Zaborski,[1] Robert Geffers,[2] Hiroshi Fujiwara,[3] Hans G. Drexler[1] and Roderick A. F. MacLeod[1]*

[1]DSMZ - German Collection of Microorganisms and Cell Cultures, Department of Human and Animal Cell Lines, Braunschweig, Germany; [2]Genome Analytics Research Group, Helmholtz Centre for Infection Research, Braunschweig, Germany and [3]First Department of Internal Medicine, Ehime University Hospital, Ehime, Japan

Acknowledgments: the authors thank cell line donors, and Prof. Dr. Reiner Siebert for commenting on the manuscript.

Correspondence: rml@dsmz.de
doi:10.3324/haematol.2017.168203

Information on authorship, contributions, and financial & other disclosures was provided by the authors and is available with the online version of this article at www.haematologica.org.

References

1. Foss FM, Zinzani PL, Vose JM, et al. Peripheral T-cell lymphoma. Blood. 2011;117(25):6756-6767.
2. Zhang Y, Xu W, Liu H, et al. Therapeutic options in peripheral T cell lymphoma. J Hematol Oncol. 2016;9:37.
3. Streubel B, Vinatzer U, Willheim M, et al. Novel t(5;9)(q33;q22) fuses ITK to SYK in unspecified peripheral T-cell lymphoma. Leukemia. 2006;20(2):313–318.
4. Martin-Subero JI, Wlodarska I, Bastard C, et al. Chromosomal rearrangements involving the BCL3 locus are recurrent in classical Hodgkin and peripheral T-cell lymphoma. Blood. 2006;108(1):401-402.
5. Almire C, Bertrand P, Ruminy P, et al. PVRL2 is translocated to the TRA@ locus in t(14;19)(q11;q13)-positive peripheral T-cell lymphomas. Genes Chromosomes Cancer. 2007;46(11):1011-1018.
6. Leich E, Haralambieva E, Zettl A, et al. Tissue microarray-based screening for chromosomal breakpoints affecting the T-cell receptor gene loci in mature T-cell lymphomas. J Pathol. 2007;213(1):99-105.
7. Shin SY, Jang S, Park CJ, et al. A rare case of Lennert's type peripheral T-cell lymphoma with t(14;19)(q11.2;q13.3). Int J Lab Hematol. 2012;34(3):328-332.
8. An J, Fujiwara H, Suemori K, et al. Activation of T-cell receptor signaling in peripheral T-cell lymphoma cells plays an important role in the development of lymphoma-associated hemophagocytosis. Int J Hematol. 2011;93(2):176-185.
9. Piccaluga PP, Agostinelli C, Califano A, et al. Gene expression analysis of peripheral T cell lymphoma, unspecified, reveals distinct profiles and new potential therapeutic targets. J Clin Invest. 117(3):823-834.
10. Gesk S, Martín-Subero JI, Harder L et al. Molecular cytogenetic detection of chromosomal breakpoints in T-cell receptor gene loci. Leukemia 2003;17(4):738-745.
11. Ehrentraut S, Schneider B, Nagel S, et al. Th17 cytokine differentiation and loss of plasticity after SOCS1 inactivation in a cutaneous T-cell lymphoma. Oncotarget. 2016;7(23):34201-34216.
12. Ehrentraut S, Nagel S, Scherr ME, et al. t(8;9)(p22;p24)/PCM1-JAK2 activates SOCS2 and SOCS3 via STAT5. PLoS One. 2013;8(1):e53767.
13. Otto C, Scholtysik R, Schmitz R, et al.. Novel IGH and MYC translocation partners in diffuse large B-cell lymphomas. Genes Chromosomes Cancer. 2016;55(12):932-943.